J. Chem. Sci. Vol. 126, No. 4, July 2014, pp. 911–917.

Interaction of meso-tetrakis(N-methylpyridinyl)porphyrin with single strand DNAs – poly(dA), poly(dT), poly(dG) and poly(dC): A photophysical study

SHARMISTHA DUTTA CHOUDHURY, JYOTIRMAYEE MOHANTY, HARIDAS PAL and ACHIKANATH C BHASIKUTTAN*

Radiation and Photochemistry Division, Bhabha Atomic Research Centre, Trombay, Mumbai 400 085, India
e-mail: bkac@barc.gov.in

MS received 29 January 2014; revised 6 March 2014; accepted 7 March 2014

Abstract. Interaction between meso-tetrakis(N-methylpyridinyl)porphyrin (TMPyP) and single strand DNA homopolymers, $(dA)_{40}$, $(dT)_{40}$, $(dG)_{40}$ and $(dC)_{40}$, has been investigated using absorption, fluorescence and circular dichroism (CD) measurements. Fluorescence intensity of TMPyP is quenched in the presence of $(dG)_{40}$ due to photo-induced electron transfer from dG to the excited TMPyP dye. Changes in the CD spectra of the polynucleotides in the presence of TMPyP are found to be quite different and depend on the nature of the nucleotide bases, whether purine or pyrimidine. Excitonic induced CD spectra is observed for TMPyP in the presence of pyrimidine homopolymers while negative induced CD is observed in the presence of purine homopolymers. Based on photophysical studies and CD spectra, we propose multiple binding modes of TMPyP with polynucleotides. TMPyP can bind to oligonucleotides both in monomer form as well as in the form of short stretches of stacked aggregates along the oligonucleotide backbone.

Keywords. TMPyP; fluorescence; ss-DNA; polynucleotide; stacking.

1. Introduction

Interaction between DNA and porphyrin derivatives has been extensively studied due to their potential applications in photodynamic therapy and as anti-cancer agents.[1–5] In many cases, DNA serves as a template for organization of porphyrin molecules into extended assemblies, providing opportunities for construction of supramolecular structures.[6–8] Among the porphyrin derivatives, meso-tetrakis(N-methylpyridinyl)porphyrin (TMPyP, chart 1) is one of the most widely investigated.[1,9–25] TMPyP is reported to be an efficient photosensitizer.[20] It interacts with human telomeric quadruplexes and stabilizes them against thermal denaturation.[21] TMPyP inhibits tumour growth by down-regulating telomerase activity.[22] Recently, TMPyP has been used as a drug delivery vehicle for anti-sense oligodeoxy nucleotides.[5] Moreover, this porphyrin derivative has also attracted considerable attention due to its molecular assembly formation with macrocyclic receptors.[24,25]

Studies on TMPyP–DNA interaction have revealed different binding modes depending on TMPyP:DNA molar ratio, nature and sequence of the DNA base pairs, length of the oligonucleotides and ionic strength of the medium. At low TMPyP:DNA ratios, TMPyP intercalates at the 5′CG3′ site of GC base pairs whereas with AT rich sequences, TMPyP binds near the minor groove.[9,12–15] As the TMPyP:DNA mole ratio increases, TMPyP molecules begin to stack outside the DNA stem.[10] Stacking of porphyrin on the DNA template leads to the appearance of a characteristic bisignate circular dichroism (CD) spectrum.[8,13] It has been found that in addition to the TMPyP:DNA molar ratios, length of the oligonucleotide also determines the preference for stacking versus other modes of binding.[11]

Although binding of porphyrins to double stranded DNA (ds-DNA) has been extensively investigated, there are very few reports on the interaction of porphyrins with single stranded DNA (ss-DNA) or ss-oligonucleotides, despite the fact that single stranded segments of DNA play important biological roles, especially in replication and transcription processes.[4,23] Further, rapid screening methods for detecting DNA damage by identifying ss-DNA, have wide applications in health-related diagnosis. So, it is evident that designing good sensors for DNA damage requires an understanding of the interaction of the dyes with both single and double stranded DNAs. Earlier Pasternack *et al*.

*For correspondence

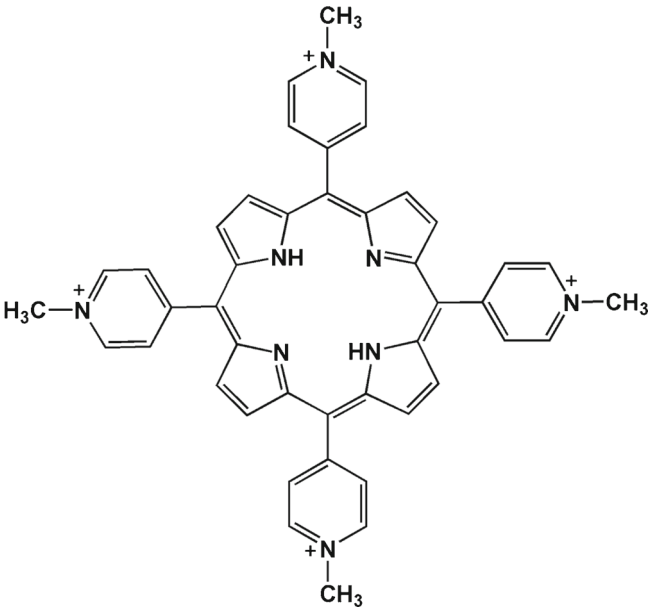

Chart 1. Chemical structure of meso-tetrakis(N-methylpyridinium)porphyrin (TMPyP).

have shown from CD studies that the metalloporphyrin, CuTMPyP, can be a useful reagent in reporting the presence of single-stranded regions in a complex nucleic acid mixture.[23] In this study, we report a systematic investigation on the interaction of TMPyP with the polynucleotides (poly(dN)), namely, $(dA)_{40}$, $(dT)_{40}$, $(dG)_{40}$ and $(dC)_{40}$, using absorption, fluorescence and CD measurements, in order to understand the mode of interaction as well as to explore the possibility of DNA template directed assembly formation of TMPyP.

2. Experimental

The tosylate form of TMPyP, from Aldrich, was converted to chloride form using anion exchange resin.[24] The NMR spectrum of TMPyP(Cl) is presented in figure S1. Concentration of TMPyP in solution was determined spectrophotometrically using the exinction coefficient, $\varepsilon_{422\,nm} = 2.26 \times 10^5\ M^{-1}\,cm^{-1}$.[11] Homopolymers (40 mers); $(dA)_{40}$, $(dT)_{40}$, $(dG)_{40}$ and $(dC)_{40}$, were obtained from Bangalore Genei, India or from IBA, Germany and concentrations of the full length species were determined using the extinction coefficients of the 40 mers, $\varepsilon_{260\,nm}$ = 554.4, 313.2, 381.24 and 266.4 $cm^2\mu mol^{-1}$, for $(dA)_{40}$, $(dT)_{40}$, $(dG)_{40}$ and $(dC)_{40}$, respectively.[26] Experiments were performed in 10 mM Tris-HCl buffer at pH 7 and ambient temperature (27°C). The TMPyP concentration was maintained at about 0.7 μM. At this concentration range self-aggregation of TMPyP is negligible.[27] Absorption spectra were recorded with a Shimadzu 160A spectrophotometer, fluorescence spectra were recorded with a Hitachi F4500 spectrofluorimeter and CD measurements were carried out with a JASCO J-815 spectrometer. Time-resolved fluorescence measurements were performed with a time-correlated single photon counting instrument (Horiba Jobin Yvon IBH, UK), using a 445 nm diode laser (~100 ps, 1 MHz repetition rate) as the excitation source and a MCP-PMT detector. Fluorescence decays were collected at magic angle (54.7°) to avoid the effect of rotational depolarization of the dye on the fluorescence lifetimes.[28,29] The DAS-6 software from IBH was used for the deconvolution analysis of the observed decays. Quality of the fits and consequently the mono- and bi-exponential nature of the decays were judged by the reduced chi-square (χ^2) values and distribution of the weighted residuals among the data channels. For a good fit, the χ^2 value was close to unity and the residuals were distributed randomly without any bias.[28,29]

3. Results and Discussion

3.1 *Steady-state absorption and fluorescence measurements*

Absorption spectrum of TMPyP shows significant changes in the presence of each of the ss-DNA homopolymers. Representative spectra for TMPyP in the presence of $(dA)_{40}$ are shown in figure 1. The most pronounced changes are observed in the Soret band of

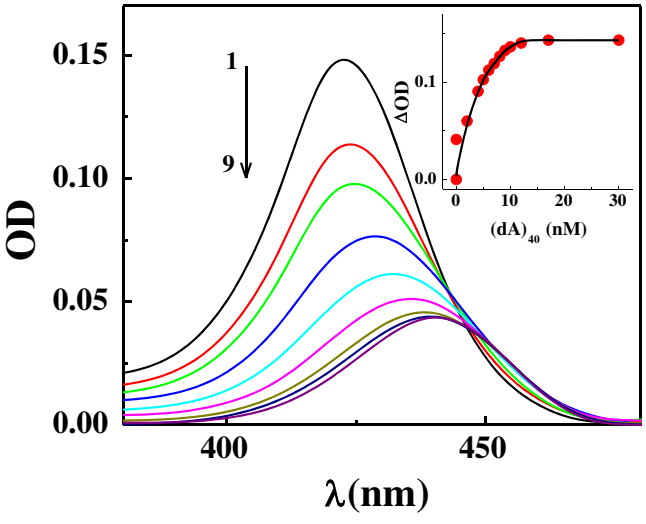

Figure 1. Absorption spectra of TMPyP (0.7 μM) in Tris buffer (pH 7) at different $(dA)_{40}$ concentrations. $[(dA)_{40}]$/nM: (1) 0, (2) 1, (3) 2, (4) 4, (5) 6 (6) 8, (7) 10, (8) 12 and (9) 30. Inset shows absorbance changes at 420 nm with different $(dA)_{40}$ concentrations.

TMPyP, so we have focused on this band for the analyses and discussions in the present study. The complete absorption spectra of TMPyP-$(dA)_{40}$ are shown in figure S2.

With increasing poly(dN) concentrations, the Soret band of TMPyP at 422 nm shows a continuous red shift (∼14–18 nm) along with a gradual decrease in the absorbance, finally reaching a limiting value at ∼20–30 nM concentration for each of the poly(dN) (figure 1 and figures S3–S5). No clear isosbestic point is observed in any of these cases, suggesting that the porphyrin binding mode is heterogeneous in nature. The binding isotherm (Inset, figure 1 and figures S3–S5) shows saturation at very low poly(dN) concentrations (∼20–30 nM). This indicates that the interaction between TMPyP and the ss-DNA homopolymers is extremely strong (binding constant $\sim 10^6$ M^{-1} for interaction of the dye with individual nucleotides in the homopolymer, Note S1). The strong binding interaction may be attributed to electrostatic attraction between the cationic TMPyP and the negatively charged poly(dN) backbone. To verify this aspect, the TMPyP–poly(dN) interaction was investigated in the presence of NaCl. It is anticipated that the accumulation of Na^+ ions near the phosphate backbone of poly(dN) can shield the negative charge of the poly(dN) backbone and hence prevent the binding of TMPyP. As expected, in a solution containing 1 M NaCl, no significant changes were observed in the Soret band absorption of TMPyP upon addition of the ss-DNA homopolymers. Alternatively, on addition of NaCl to the TMPyP-poly(dN) complexes, the absorption spectrum was found to revert to the initial spectrum of free TMPyP, suggesting disruption of the TMPyP-poly(dN) interaction (figure S6).

In the present experimental conditions, the TMPyP:poly(dN) molar ratio is greater than 1.0. Considering the highest concentration of the poly(dN) used (30 nM) and a typical TMPyP concentration of ∼0.7 μM as used in the present cases, one TMPyP molecule is available per two nucleobases in the polynucleotide chain. So, binding and stacking of multiple TMPyP molecules outside the poly(dN) stem appears to be quite possible. In fact, considerable decrease in the absorbance of TMPyP in the presence of all the ss-DNA homopolymers (∼80% hypochromicity), suggests strong interaction of TMPyP with the π-systems of the nucleotide bases and/or among the π-systems of neighbouring porphyrins themselves. It may be mentioned that the extent of red shift and the hypochromicity in the Soret band of TMPyP is observed to be much larger in the present cases, in comparison to the values reported previously for ds-oligonucleotides, at low TMPyP:DNA base ratios. For example, in the interaction of TMPyP with poly(dA).poly(dT), around 8 nm red shift and 38% hypochromicity was observed; whereas for TMPyP-poly(dG).poly(dC) system, the red shift and hypochromism was about 20 nm and 58%, respectively.[13] Differences in the interactions of TMPyP with the two different ds-oligonucleotides were ascribed to the preference of the dye for intercalation with GC base pairs and groove binding for AT base pairs.[13] In the present case, however, the extent of hypochromicity is similar for all the hompolymers studied. So, it is possible that the large hypochromicity arises from the interaction among the π-systems of neighbouring porphyrins due to the formation of assemblies with multiple dyes that are bound to the poly(dN) backbone.

For a better understanding, we investigated the effect of poly(dN) on the fluorescence spectra of TMPyP. Fluorescence spectrum of TMPyP is broad and structureless. This spectral broadening is the result of two effects: first, intramolecular rotation of the pyridinium groups of TMPyP; and second, the mixing of the first excited singlet state of TMPyP with a close lying intramolecular charge transfer (CT) state involving partial transfer of charge from the core of the porphyrin to the electron-deficient pyridinium groups.[27]

Significant changes are observed in the fluorescence spectra on addition of the ss-DNA homopolymers. In the presence of, $(dA)_{40}$, $(dT)_{40}$ or $(dC)_{40}$, fluorescence spectrum of TMPyP resolves into two bands with maxima around 660 and 720 nm, which correspond to the Q(0,1) and the Q(0,0) transitions.[24,30] Representative fluorescence spectra for TMPyP in the presence of $(dT)_{40}$ are shown in figure 2. The observed spectral changes can be attributed to the binding of the dye to the phosphate backbone of the poly(dN), which prevents intramolecular rotation of the pyridinium groups of TMPyP and thus improves the spectral resolution. Moreover, compensation of the charges on the pyridinium groups by the negatively charged phosphate groups of poly(dN) prevents the intramolecular CT in TMPyP. Inhibition of CT from the porphyrin core to the pyridinium groups, changes the energy level of the intramolecular CT state of TMPyP and inhibits its mixing with the first excited singlet state, thus leading to increased spectral resolution.[20]

An apparent reduction in the fluorescence intensity of TMPyP is noticed on addition of the polynucleotides, $(dA)_{40}$, $(dT)_{40}$ or $(dC)_{40}$. Since, absorbance of TMPyP also decreases in the presence of the polynucleotides, it is necessary to correct the corresponding differences in optical density (OD) at the excitation wavelength

(445 nm) in order to delineate the effect of reduced absorbance on the fluorescence spectra. On correcting the observed fluorescence spectra by OD normalization, it is found that fluorescence intensity in the presence of these polynucleotides is actually somewhat greater than that of the free porphyrin (Inset, figure 2). This is expected because the bound porphyrin should have reduced molecular mobility, which should decrease the non-radiative deactivating channels and hence increase the fluorescence yield of TMPyP.

In the presence of $(dG)_{40}$, the changes in fluorescence spectra of TMPyP (figure 3) are quite different from that observed in the presence of the other poly(dN). In this case, although the broad emission spectrum of the dye resolves into two bands, it is not as marked as in the case of the other three polynucleotides. Moreover, fluorescence intensity of TMPyP is clearly quenched in the presence of $(dG)_{40}$, even after correction by normalizing the OD at the excitation wavelength (Inset, figure 3). It is reported that TMPyP forms a charge transfer complex with the nucleotide, dGTP, involving photo-induced electron transfer (PET) from dGTP to the porphyrin dye.[19,20] The free energy change (ΔG^0) for PET from the nucleotides to the excited TMPyP dye, can be expressed according to the Rehm Weller relation[31] as

$$\Delta G^0 = E\left(dN/dN^+\right) - E\left(TMPyP/TMPyP^-\right) - E_{00} + w \quad (1)$$

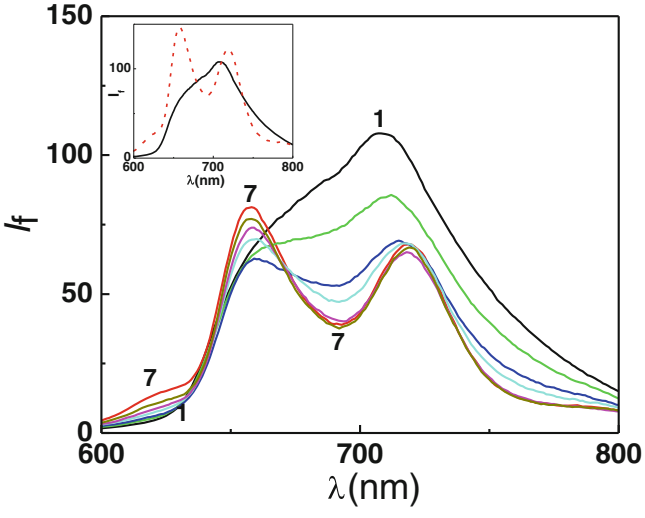

Figure 2. Steady-state fluorescence spectra of TMPyP (0.7 μM) in Tris buffer (pH 7) at different $(dT)_{40}$ concentrations, $[(dT)_{40}]$/nM: (1) 0, (2) 1, (3) 2, (4) 3, (5) 4, (6) 6 and (7) 10. Excitation wavelength was 445 nm. Inset shows the spectra corresponding to (1), solid line and (7), dotted line, after correcting the observed fluorescence intensities by OD normalization at the excitation wavelength.

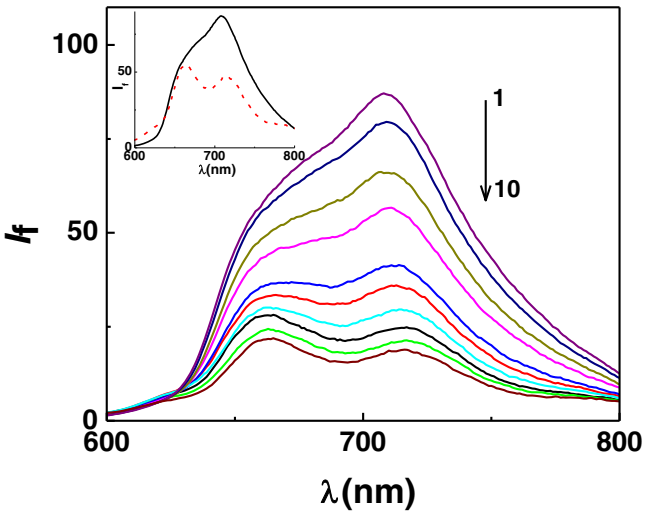

Figure 3. Steady-state fluorescence spectra of TMPyP (0.7 μM) in Tris buffer (pH 7) at different $(dG)_{40}$ concentrations, $[(dG)_{40}]$/nM: (1) 0, (2) 1, (3) 2, (4) 3, (5) 4, (6) 5, (7) 6, (8) 7, (9) 8 and (10) 10. Excitation wavelength was 445 nm. Inset shows the spectra corresponding to (1), solid line and (7), dotted line, after correcting the observed fluorescence intensities by OD normalization at the excitation wavelength.

Here, $E(dN/dN^+)$ and $E(TMPyP/TMPyP^-)$ are the oxidation and reduction potentials of the nucleotide and TMPyP, respectively, E_{00} is the excitation energy of TMPyP in the S_1 state and w is the coulomb energy. Redox potentials of dA, dT, dG and dC are reported to be 1.94, 1.73, 1.53 and 1.88 V, respectively.[19] Considering that the reduction potential of TMPyP is −0.23 V and its excited singlet state energy (E_{00}) is 1.83 eV, a thermodynamically favourable PET is feasible only from dG to TMPyP.[19] No PET can be expected from dA, dT or dC. So the fluorescence quenching of TMPyP in the presence of $(dG)_{40}$ can be clearly assigned to PET from the guanine residues of $(dG)_{40}$ to the excited porphyrin.

3.2 *Time-resolved fluorescence measurements*

Figure 4 shows representative decay traces of TMPyP alone and in the presence of $(dA)_{40}$ and $(dG)_{40}$. Decay parameters in the presence of each of the poly(dN) are presented in table 1. In the absence of polynucleotides, fluorescence decay trace for TMPyP at 660 nm can be fitted to a mono-exponential function with a time constant of about 5 ns, which corresponds to the reported excited-state lifetime of TMPyP.[24] In the presence of $(dA)_{40}$, $(dT)_{40}$ and $(dC)_{40}$, fluorescence decay of TMPyP becomes slower and the decay traces can be fitted predominantly with a long lifetime component in the range of ~9–11 ns. This long lifetime component is assigned to the polynucleotide-bound TMPyP

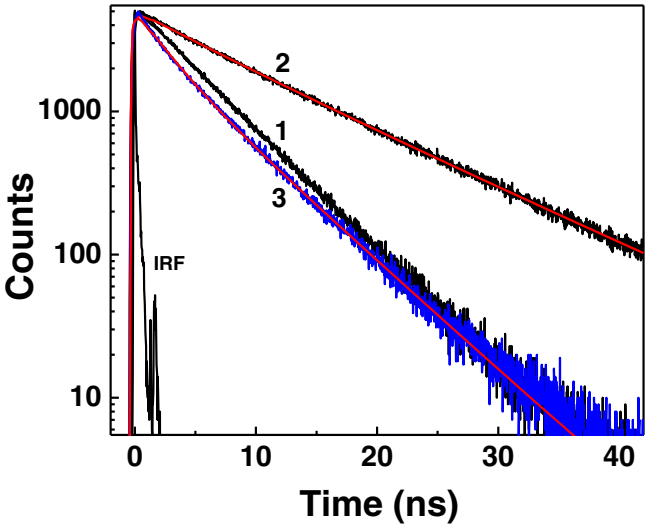

Figure 4. Fluorescence decay traces at 660 nm for TMPyP alone (1) and TMPyP in the presence of $(dA)_{40}$ (2), $(dG)_{40}$ (3). The TMPyP concentration was 0.7 μM.

molecules. Increase in the fluorescence lifetime of TMPyP on binding to poly(dN) is expected due to restriction on the intramolecular motions of the bound dye and consequently to the reduction in the nonradiative decay rate of TMPyP. The small contribution (∼9–14%) from a shorter lifetime component, ∼1.7–1.9 ns (table 1), observed in the cases of $(dT)_{40}$ and $(dC)_{40}$ strands may be due the contribution from aggregated TMPyP, that are formed along the negatively charged backbone of poly(dN) (see discussion on the circular dichroism measurements). Better correlation of the bi-exponential fitting of the fluorescence decay traces of TMPyP in the presence of $(dT)_{40}$ and $(dC)_{40}$ are shown in figures S7 and S8, respectively (SI). In contrast to the increase in the fluorescence lifetime of TMPyP in the presence of $(dA)_{40}$, $(dT)_{40}$ and $(dC)_{40}$, fluorescence decay time of TMPyP becomes shorter in the case of $(dG)_{40}$ (figure 4). This is in accordance with the fluorescence quenching of TMPyP in the presence of $(dG)_{40}$ and is attributed to PET from dG to TMPyP.[19,20]

Table 1. Fluorescence decay parameters for TMPyP in the presence of the polynucleotides (poly(dN)) measured at 660 nm. A_i values correspond to the fractional contribution of each decay time to the steady state intensity.

Poly(dN)	Fitted decay parameters			
(10 nM)	A_1(%)	τ_1 (ns)	A_2(%)	τ_2(ns)
–	100	5.1		
$(dA)_{40}$	100	10.6	–	–
$(dT)_{40}$	86	9.2	14	1.9
$(dC)_{40}$	91	9.4	9	1.7
$(dG)_{40}$	75	5.2	25	2.5

[a]Fractional contributions are estimated as $A_i = a_i\tau_i / \sum_i a_i\tau_i$, for the bi-exponential intensity decays,[28] $I(t) = \sum_i a_i \exp(-t/\tau_i)$.

3.3 *Circular dichroism measurements*

For a better picture of TMPyP-poly(dN) interaction, we carried out circular dichroism (CD) measurements. The CD spectra of the pure polynucleotides match well with the reported spectra for ss-oligomers.[23,32] Addition of TMPyP, leads to considerable changes in the spectra, which indicates a strong interaction of the dye with all the polynucleotides. Quite notably, however, these changes are found to depend on the nature of the bases that constitute the polynucleotide (i.e., whether purine or pyrimidine). Representative spectra for TMPyP-$(dA)_{40}$ and TMPyP-$(dC)_{40}$ are shown in figure 5.

For the pyrimidine polynucleotides, $(dC)_{40}$ and $(dT)_{40}$, a large change in the conformation of the polynucleotides (200–350 nm region) can be observed in the presence of TMPyP (figures 5a and S9). Conformational change of the purine polynucleotides, $(dA)_{40}$ and $(dG)_{40}$, is comparatively less prominent (figures 5b and S10). Occurrence of induced CD in the Soret band of TMPyP (∼400–500 nm region) is observed in all the polynucleotides, further supporting the binding of TMPyP to the polyneucleotide backbone, but again, the induced CD spectra are different for the purine and pyrimidine polynucleotides. A clear bisignate (or excitonic) induced CD spectrum is observed for the interaction of TMPyP with the pyrimidine polynucleotide, $(dC)_{40}$ (figure 5a) with a negative peak at approximately 425 nm and a positive peak at approximately 444 nm. This feature suggests the stacking of TMPyP along the oligonucleotide backbone of $(dC)_{40}$.[8,11,13,23]

The bisignate induced CD spectrum that is characteristic of stacking interaction is also observed to some extent for TMPyP-$(dT)_{40}$ (figure S9). On the other hand, for the interaction of TMPyP with the purine homopolymers, TMPyP-$(dA)_{40}$ (figure 5b) and TMPyP-$(dG)_{40}$ (figure S10), a negative induced CD is observed in the 400-500 nm region. Appearance of a negative induced CD band is typical of porphyrin intercalators.[16] So, it appears that the bound TMPyP intercalates with the π-systems of the purine nucleotide bases in the case of $(dA)_{40}$ and $(dG)_{40}$ and prefers a stacking interaction along the oligonucleotide backbone for the pyrimidine homopolymers, $(dC)_{40}$ and $(dT)_{40}$. This is a very interesting finding and to the best of our knowledge has not been reported in the literature so far. This

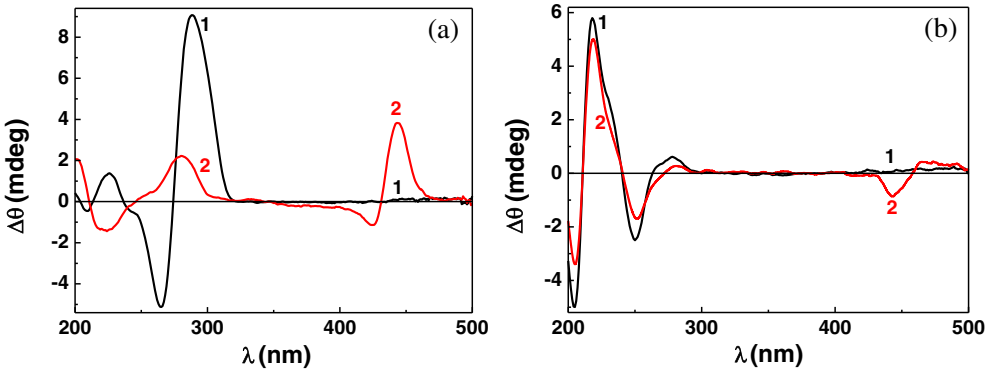

Figure 5. CD spectra of (**a**) $(dC)_{40}$ alone (2 μM) (1) and in the presence of TMPyP (40 μM) (2) and (**b**) $(dA)_{40}$ alone (1 μM) (1) and in the presence of TMPyP (23 μM) (2).

stacking interaction for the homopolymers also explains the small contribution from a short decay component (1.7–1.9 ns, 9–14%, (table 1) observed in the fluorescence decay traces recorded at 660 nm in the $(dC)_{40}$ and $(dT)_{40}$ strands.

The CD spectra in conjunction with absorption and fluorescence measurements help in our understanding of the interaction between TMPyP and ss-DNA homopolymers. Changes in the absorption and fluorescence spectra of TMPyP in the presence of $(dA)_{40}$, $(dT)_{40}$, $(dG)_{40}$ or $(dC)_{40}$ are quite similar, except the fluorescence quenching observed with $(dG)_{40}$ in contrast to the fluorescence enhancement observed with the other polynucleotides. So, it is not possible to distinguish between the interactions of TMPyP with the various homopolymers on the basis of absorption and fluorescence studies alone. CD measurements, however, reveal that there are differences in the interactions of TMPyP with the homopolymers, $(dA)_{40}$, $(dT)_{40}$, $(dG)_{40}$ or $(dC)_{40}$, leading to different changes in the conformations of the single strand and in the nature of the induced CD in the Soret band region of TMPyP. The present results indicate that the ss-DNA homopolymers can act as scaffolds for the aggregation of TMPyP by simple non-covalent electrostatic interactions. It is interesting to note that the stacking of the porphyrin molecules can be induced at very low (nano molar) concentrations of the poly(dN). Such template-directed organized assemblies of chromophoric molecules may have implications in the design of photofunctional materials for various applications such as light harvesting or molecular photovoltaics.

4. Conclusions

The porphyrin dye, TMPyP, has strong electrostatic interaction with the ss-DNA homopolymers, $(dA)_{40}$, $(dT)_{40}$, $(dG)_{40}$ and $(dC)_{40}$. Absorption spectral changes of TMPyP are very similar in the presence of all the homopolymers studied, irrespective of the nature of the nucleotides. Fluorescence spectra of TMPyP resolves into two bands with marginal enhancement in fluorescence intensity, in the presence of $(dA)_{40}$, $(dT)_{40}$ and $(dC)_{40}$. In the case of $(dG)_{40}$, however, photoinduced electron transfer from guanosine bases to the porphyrin molecule leads to fluorescence quenching and a decrease in the fluorescence lifetime of TMPyP, though the fluorescence spectra resolve into two bands similar to that in the cases of other polynucleotides. Changes in the CD spectra of the polynucleotides in the presence of TMPyP are interestingly, quite different and depend on the nature of the nucleotide bases, whether purine or pyrimidine. Excitonic induced CD spectra is observed for TMPyP in the presence of the pyrimidine homopolymers while negative induced CD is observed in the presence of the purine homopolymers. Based on photophysical studies and the CD spectra, we propose multiple binding modes of TMPyP with the polynucleotides. TMPyP can bind to oligonucleotides both in monomer form as well as in the form of short stretches of stacked aggregates along the oligonucleotide backbone. Thus, the ss-DNA homopolymers may act as suitable templates for the formation of TMPyP assemblies through non-covalent electrostatic interactions.

Supplementary Information

Figures S1–S10 are given as supplementary material. For details, see www.ias.ac.in/chemsci.

Acknowledgements

We thank Dr. (Mrs.) Lata Panicker, (Solid State Physics Division), Bhabha Atomic Research Centre (BARC)

and Dr. N Barooah, (Radiation & Photochemistry Division), BARC, for helping with the CD measurements. We thank for the support received from our host institute.

References

1. Tada-Oikawa S, Oikawa S, Hirayama J, Hirakawa K and Kawanishi S 2009 *Photochem. Photobiol.* **85** 1391
2. Patito I A, Rothmann C and Malik Z 2001 *Biol. Cell* **93** 285
3. Kolarova H, Macecek J, Nevrelova P, Huf M, Tomecka M, Bajgar R, Mosinger J and Strnad M 2005 *Toxicol. in Vitro* **19** 971
4. Bustamante C, Currieri S, Pasternack R F, Purello R and Riazzarell E 1994 *Biopolymers* **34** 1099
5. Benimetskaya L, Takle G B, Vilenchik M, Lebedeva I, Miller P and Stein C A 1998 *Nucl. Acids Res.* **26** 5310
6. Fendt L-A, Bouamaied I, Thöni S, Amiot N and Stulz E 2007 *J. Am. Chem. Soc.* **129** 15319
7. Wagenknecht H-A 2009 *Angew. Chem. Int. Ed.* **48** 2838
8. Pasternack R F and Giannetto A S 1991 *J. Am. Chem. Soc.* **113** 7799
9. Sehlstedt U, Kim S K, Carter P, Goodisman J, Vollano J F, Norden B and Dabrowiak J C 1994 *Biochemistry* **33** 417
10. Park T, Shin J S, Han S W, Son J-K and Kim S K 2004 *J. Phys. Chem. B* **108** 17106
11. Park T, Kim J M, Han S W, Lee D-J and Kim S K 2005 *Biochim. Biophys. Acta* **1726** 287
12. Guliaev A B and Leontis N B 1999 *Biochemistry* **38** 15425
13. Lee S, Jeona S H, Kim B-J, Han S W, Jang H G and Kim S K 2001 *Biophys. Chem.* **92** 35
14. Marzilli L G, Banville D L, Zon G and Wilson W D 1986 *J. Am. Chem. Soc.* **108** 4188
15. Lee Y-A, Lee S, Cho T-S, Kim C, Han S W and Kim S K 2002 *J. Phys. Chem. B* **106** 11351
16. Lee Y-A, Kim J-O, Cho T-S, Song R and Kim S K 2003 *J. Am. Chem. Soc.* **125** 8106
17. Lee S, Lee Y-A, Lee H M, Lee J Y, Kim D H and Kim S K 2002 *Biophys. J.* **83** 371
18. Kim J-O, Lee Y-A, Yun B H, Han S W, Kwag S T and Kim S K 2004 *Biophys. J.* **86** 1012
19. Jasuja R, Jameson D M, Nishijo C K and Larsen R W 1997 *J. Phys. Chem. B* **101** 1444
20. Chirvony V S, Galievsky V A, Kruk N N, Dzhagarov B M and Turpin P-Y 1997 *J. Photochem. Photobiol. B: Bio.* **40** 154
21. Wheelhouse R T, Sun D, Han H, Han F X and Hurley L H 1998 *J. Am. Chem. Soc.* **120** 3261
22. Grand C L, Han H, Munoz R M, Weitman S, Von Hoff D D, Hurley L H and Bearss D H 2002 *Mol. Cancer Ther.* **1** 565
23. Pasternack R F, Brigandi R A, Abrams M J, Williams A P and Gibbs E J 1990 *Inorg. Chem.* **29** 4483
24. Mohanty J, Bhasikuttan A C, Dutta Choudhury S and Pal H 2008 *J. Phys. Chem. B* **112** 10782
25. (a) Barooah N, Bhasikuttan A C, Sudarsan V, Dutta Choudhury S, Pal H and Mohanty J 2011 *Chem. Commun.* **47** 9182; (b) Liu Z D, Zhao H X and Huang C Z 2012 *PLoS ONE* **7** e50367. DOI: 10.1371/journal.pone.0050367Z
26. Kibbe W A 2007 *Nucl. Acids Res.* **35** W43
27. Vergeldt F J, Koehorst R B M., Hoek A V and Schaafsma T J 1995 *J. Phys. Chem.* **99** 4397
28. Lakowicz J R 2006 *Principles of fluorescence spectroscopy* (New York: Springer)
29. O'Connor D V and Phillips D 1984 *Time correlated single photon counting* (New York: Academic Press)
30. Kalyanasundaram K 1984 *Inorg. Chem.* **23** 2453
31. Rehm D and Weller A 1970 *Isr. J. Chem.* **8** 259
32. Marck C and Thiele D 1978 *Nucleic Acids Res.* **5** 1017